

INVITED ARTICLE



Effect of internal energy depletion on active nematic texture and dynamics

Fereshteh L. Memarian and Linda S. Hirst

Department of Physics, University of California, Merced, CA, USA

ABSTRACT

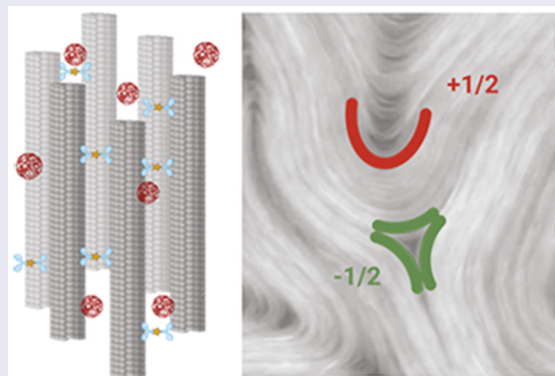
Active nematics represent a relatively new class of materials with liquid crystalline properties that rely on an energy source to maintain their structure and dynamics. In this paper, we focus on the well-known microtubule-kinesin-based active nematic, powered by chemical energy as ATP (Adenosine triphosphate), and report on how ATP depletion impacts active nematic defect dynamics and texture. Using fluorescence microscope video imaging, we measure the time averaged mean defect separations and root mean square velocities of the active flows as a function of time. We also characterise textural changes and the growth of void space in the network after ATP depletion using an image binarization technique.

ARTICLE HISTORY

Received 6 March 2023

KEYWORDS

Active nematic; active matter; microtubule; molecular motors; ATP



Introduction

Active nematics are one of the most exciting new forms of liquid crystal to emerge in recent years. Similar to the conventional nematic phase, active nematics exhibit local orientational order, but they exist in an intrinsically out-of-equilibrium state. The nematic structure of the phase is driven by an energy consuming process, which acts to maintain alignment and drive global fluid dynamics, including defect creation and annihilation. A wealth of recent theoretical and computational work has explored the active nematic phase, whereas experimental realisations have been somewhat limited and have focused on constructing the phase from micron-scale biological assemblies. The experiments reported here use an active nematic phase formed from microtubules (protein-based biofilaments) and kinesin motor proteins. These motors produce active stresses between parallel microtubules in the presence of ATP (Adenosine tri phosphate), driving local filament

alignment and the formation of topological defects (Figure 1(a)).

The first experimental example of an active nematic was reported by Sanchez et al. [1], adapting an earlier *in vitro* experiment [2] in which clusters of kinesin motors were coupled to a microtubule network to produce a dilute active filamentous phase. By confining the active fluids to a thin layer geometry, and thus forcing the material to a high density, spontaneous nematic ordering emerged. This nematic phase exhibits moving $+1/2$ and $-1/2$ topological defects (Figure 1(b)). Recently, several experimental groups [1,3–6] worked with this active phase in efforts to understand and control its fundamental characteristics. The material has also attracted a great deal of theoretical attention [7–9] with several studies focusing on the phenomenon of so-called active turbulence – a dynamic state in which the active fluid produces self-driven chaotic flows [10,11]. The nematic state of the microtubule-kinesin-based fluid should not be considered a traditional liquid

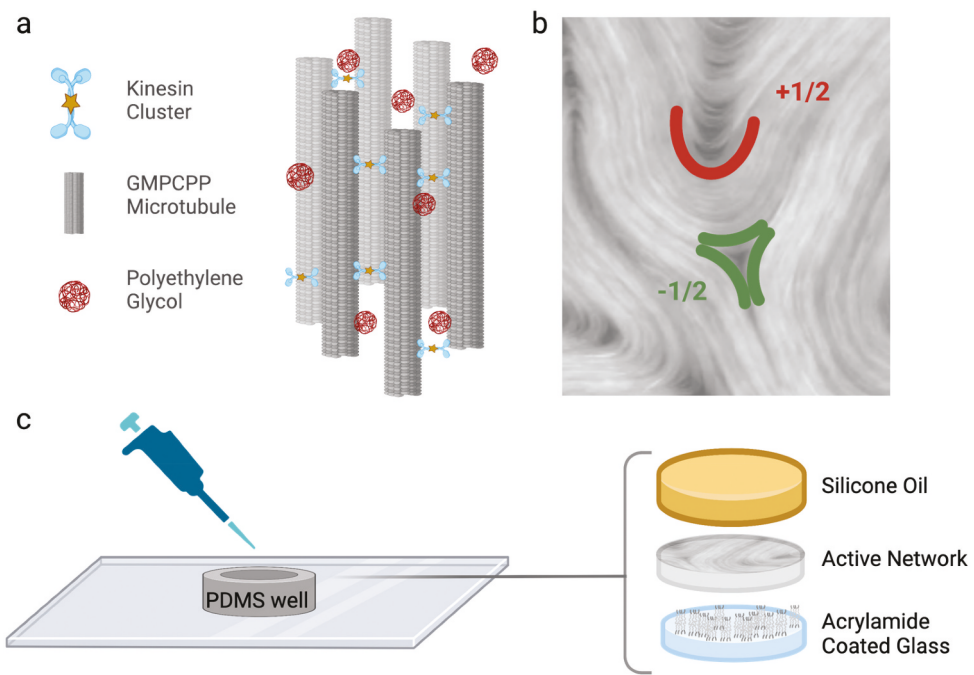


Figure 1. (Colour online) a) Cartoon representing the building blocks of the active phase, kinesin clusters bound to microtubules. b) Fluorescence microscope image of the active phase showing a typical texture with positive (red) and negative (green) topological defects highlighted. c) Schematic of active nematic preparation, the active network layer is confined in a PDMS well for microscopy.

crystal, in the sense that the order of the phase is not governed by thermodynamics and free energy minimisation. Rather, the active nematic state is maintained by continual injection of energy (via ATP hydrolysis at the kinesin motors) at the molecular level and thus is always out of equilibrium in the traditional sense.

Despite the high degree of interest in the active nematic phase, it can be challenging for experimentalists to enter the field. The active network is composed of biological proteins which can be expensive to obtain and challenging to handle. Our group recently published detailed protocols for preparing microtubule-based active nematics in different experimental geometries [12]. Other groups have constructed a similar phase from the protein filament F-actin and myosin motors, and from doping traditional chromonic liquid crystal with motile bacteria [13]. There are, however, currently no known active liquid crystals composed purely of fully synthetic liquid crystal molecules and colloids – such a development would be of great significance to the field.

One challenge in preparing an active nematic phase from biological components is to maintain the rate of activity over long time periods. The power source for this phase is ATP, and the local velocity of microtubule motion depends directly on ATP concentration. ATP molecules drive the walking motion of kinesin [14] in 8 nm steps towards the positive end of the microtubule

(Figure 1(a)). Once the ATP becomes depleted, the network velocities and the active length-scale of the fluid change dramatically. Such time-dependent changes can become problematic for long time-scale experiments. In the following sections, we present data collected using fluorescence microscopy. We quantify the effects of ATP depletion on the active nematic phase, calculating mean topological defect separations over long time periods and network root-mean-squared velocities. The averaged defect separation is used to calculate an active length-scale, and the effects of this changing length-scale can also be seen in the phase texture. Additional textural changes are also observed beyond the point of total ATP depletion, when the network stops flowing actively.

Methods

The active nematic used in these experiments was prepared as previously reported by our group. For our most recent detailed methods, refer to Memarian et al. [12]. To form the active phase, fluorescently tagged 2 µm polymerised microtubules are combined with kinesin motor clusters. The microtubules are polymerised from tubulin in the presence of Guanosine-5'-[(α,β)-methylene]triphosphate, sodium salt (GMPCPP). This slowly hydrolysable analog of Guanosine triphosphate (GTP) produces microtubules that are three times stiffer

than microtubules polymerised using GTP [15]. Short, stiff microtubules are more rod-like, and thus favourable for nematic-phase formation, promoting liquid crystalline ordering.

The kinesin clusters are formed using a biotin-streptavidin linkage. Kinesin binds to microtubules and, in the presence of ATP, causes neighbouring microtubules of opposing polarity to slide relative to each other in a shearing motion. This molecular-scale active stress drives the dynamics of the active nematic phase. To help promote microtubule condensation into bundles via depletion forces, we include 20 kDa Polyethylene glycol in the solution. An antifade solution (prepared from Glucose, Glucose Oxidase, Catalase, and DTT (dithiothreitol)) is added to prevent photobleaching during imaging. An essential component of the active phase is ATP. To generate a directional walking motion along a microtubule, a kinesin motor must sequentially unbind and bind its two binding domains (the 'feet'). To release kinesin from the microtubule, ATP is necessary. In a typical experiment, we also include pyruvate kinase/lactic dehydrogenase (PKLDH) for ATP regeneration [12] to prolong motor activity over several hours. The ATP is added right before imaging to activate the system and generate the active network.

Active phase assembly

The active network is typically sandwiched between two fluids (water and oil) to promote high enough densities for nematic-phase formation (Figure 1(c)). In this set of experiments, we constructed a simple PDMS well with a diameter of approximately 5 mm. To make the PDMS well, the elastomer base and elastomer agent are mixed in a ratio of 10:1, degassed under vacuum for 1 h, then cured in an oven for 4 h at 60°C. The glass substrate is coated with an acrylamide polymer brush to prevent proteins from sticking to the glass slide and make the glass slide hydrophilic. The PDMS well is glued to the acrylamide-coated glass slide with UV glue. We add 60 μ L of silicone oil with 685.6 (± 11.7) mPa.s viscosity to the well, then inject 0.75 μ L of active network solution under the oil layer. After 1 h, the active nematic network forms a quasi-2D phase.

Imaging

The microtubules used in this work were fluorescently labelled using Alexa 647 by incorporating 4% labelled tubulin into the unlabelled tubulin during polymerisation. This labelling method allows a clear visualisation of the microtubule bundles in the dynamic active

nematic texture. The material is imaged using a Leica DM 2500 P fluorescence microscope in reflection mode with a Hamamatsu ORCA-flash 4.0 LT CMOS camera, and 5 \times objective lens. Image sequences were taken with a 500 ms exposure time and recorded every 2 s.

Image analysis

Video sequences of 2048 \times 2048-pixel images were recorded using a fluorescence microscope at different times for up to 45 h. The images show nematic-like organisation of the microtubules and characteristic +1/2 and -1/2 moving topological defects. Figure 2(a-c) shows three characteristic images at 1 h, 3 h and 6 h in a video sequence. To calculate the time-dependent defect counts for a video of N frames, the frame was divided into four sub-areas of 800 \times 800 pixels. The total defects in each sub-area were then manually counted (+1/2 and -1/2 defects separately) and time averaged over three adjacent frames in the image sequence (over 6 mins). This method allowed us to measure the total defect number in several different areas of the total image over a long time-period accurately, while minimising counting errors due to small numbers of defects in a particular frame. Defect counts for each of the four sub-regions collected at the same time points were then averaged to produce the graphs shown in Figure 2(d,e). To compare these results to the active length-scale (a quantity proportional to the mean defect separation), we adopted a simple method to determine the mean defect separation as, $l_a = \sqrt{\frac{1}{n_d}}$, where n_d is the areal density, and plotted the results as a function of time Figure 2(f).

To calculate the root mean squared velocity of the active phase (v_{rms}), we used the Particle Image Velocimetry (PIVLab) application with Matlab to extract time-dependent velocity maps of the active flows [16,17].

Briefly, we imported a tiff sequence of images into the software, and calculated x and y components of the image velocity from frame to frame using a grid of 4 \times 4 pixel squares. Tracer particles were not necessary as the software is able to compute velocity field from the moving fluorescent microtubules. For this analysis, all image frames processed were the same size and the videos all contained the same number of frames.

From these PIV velocity maps, it was possible to extract v_{rms} as a function of time. Figure 3 shows v_{rms} for the active phase at four different timepoints, starting from $t = 0$. In addition to the distinct changes in mean defect separation presented in Figure 2(d), this data demonstrates the dramatic slowdown in the active phase over a period of 4 h. Such behaviour is very

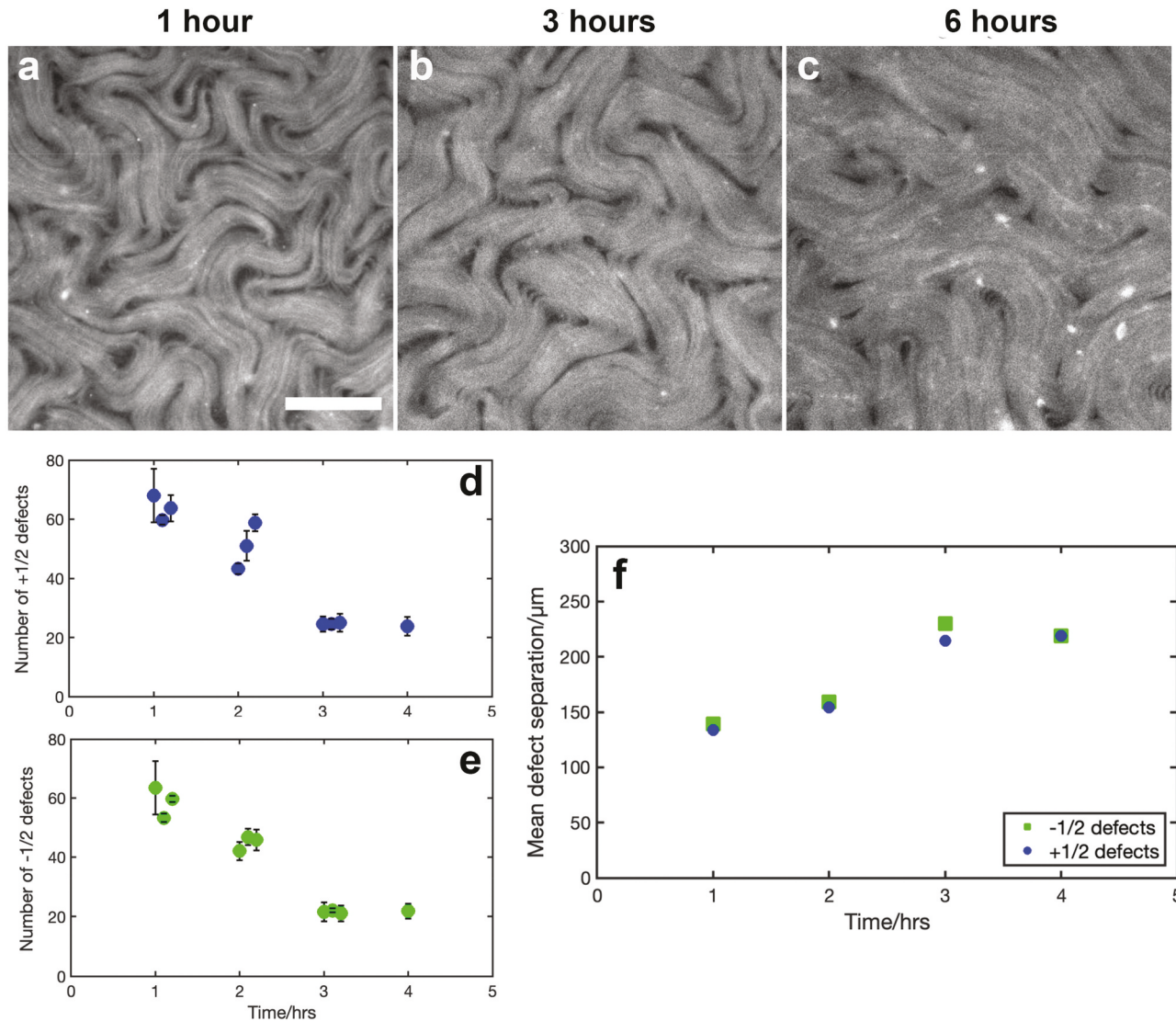


Figure 2. (Colour online) (a-c) Representative fluorescence microscope images of three active nematic texture recorded on the same microscope slide over a 6-h time period. Variation in the average defect separation is apparent (bar – 200 μ m). Time varying positive (d) and negative (e) topological defect counts and calculated mean defect separation (f) are shown.

consistent with our expectations as previous papers reported the effect of ATP concentration on single microtubule velocities (RSC) and on v_{rms} for the collective motion of the active phase [10].

Textural changes after ATP depletion

After 4 h of observation, the characteristic active nematic dynamics were no longer present; however, we continued to observe subtle textural changes in the system for up to 45 h. Comparing the 6-h timepoint to the 45-h time point in Figure 4(a-d), we can see that the black voids or gaps in the network have become larger. These voids between microtubule bundles increase in area over time and the active nematic appears to undergo localised contraction.

To quantify this ageing effect in Figure 4(b), we calculated the number of dark pixels on each image using a simple binarization method. We used ImageJ/FIJI to process the raw images. The overall image brightness decreases over time over the lifetime of the experiment so first each image was adjusted to be visually similar using the brightness tool in FIJI. A background subtraction was applied to the images, and then the Gaussian blur filter (radius of 2 pixels) was applied. The images were binarized using the Otsu filter with a threshold determined by the peak of the intensity histogram. Once the images were binarized, the histogram tool was used to extract the ratio of dark to light pixels. Figure 4(e) shows the plotted void area ratio as a function of time. We note that the binarization method we used does appear to overestimate the area

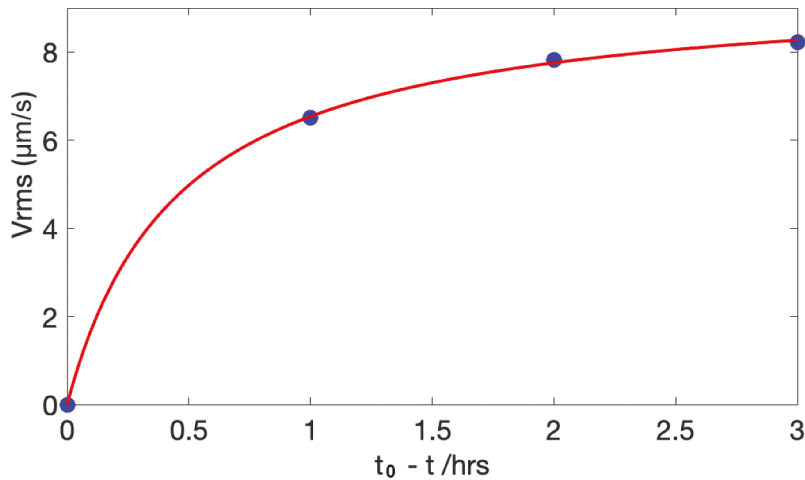


Figure 3. (Colour online) Plot displaying the calculated root mean squared velocity of the active network at different time points, showing the effects of ATP depletion. The data is fitted to a Michaelis-Menten kinetic model $v_{\text{rms}} = v_{\text{rmsmax}}[t_0 - t]/(t_0 - t + k_m)$. Where t_0 is the time when motion is observed to stop (4 hrs).

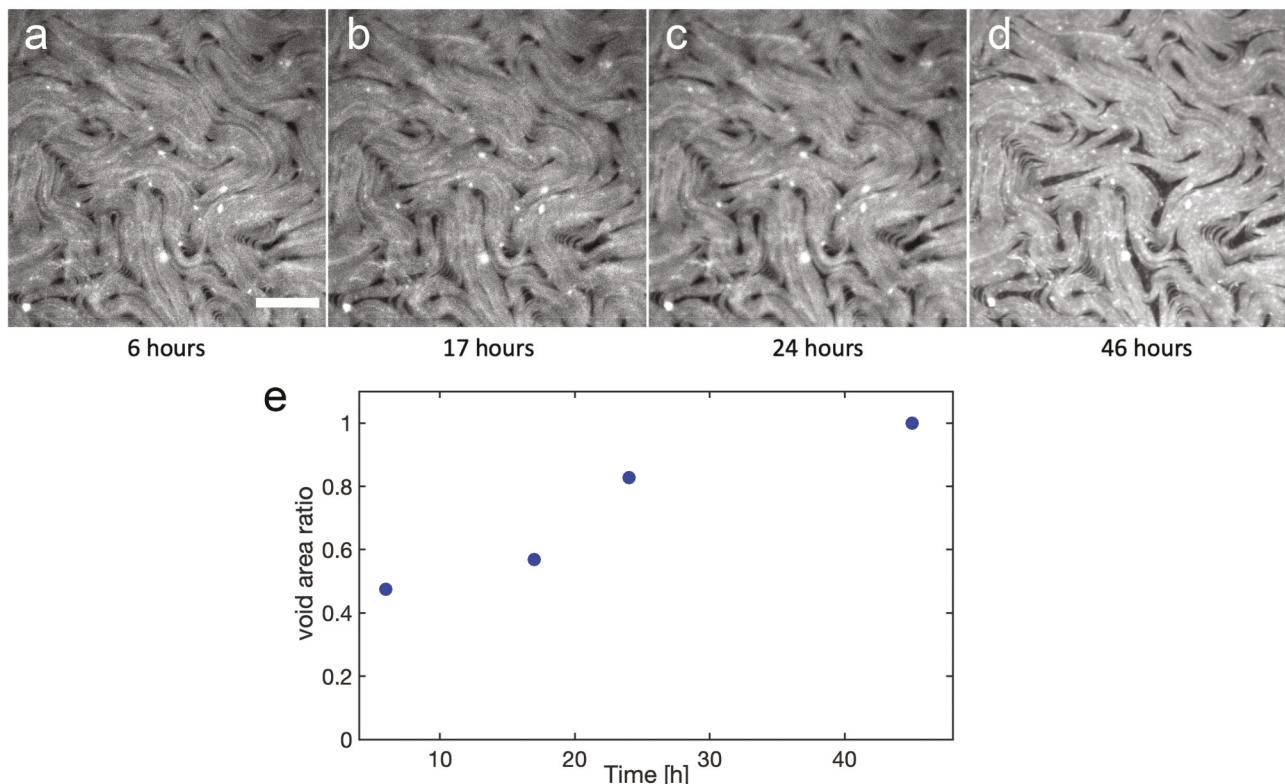


Figure 4. (Colour online) (a) Typical image sequence for the active nematic post ATP depletion (scalebar = 200μm). (b) Plot showing the change in the ratio of void to occupied space in the images as a normalized area ratio of binarized dark/light pixels.

of dark pixels in the images compared to simple visual inspection. However, a clear trend towards increasing void area is seen. Complications in applying a consistent quantitative method arise due to the nature of the material being imaged. The bundles are not uniformly distributed in the natively aligned phase but instead have a fractal density distribution [18] with the smallest

filaments below the resolution limit of the imaging technique. This makes the background subtraction step in image processing for binarization very challenging.

We expect that the ageing phenomenon seen in the network is due to a gradual increase in the degree of microtubule crosslinking by the kinesin clusters. In an

active network, ATP is required for kinesin unbinding, which facilitates the stepping motion. However, the presence of ATP is not required for kinesin binding. Thus, as ATP becomes depleted from the system, we can expect any free unbound kinesin clusters to eventually bind to the microtubules, acting as crosslinkers. This increased cross-linking appears to locally condense the bundles, and as a result, increases the area of the large voids.

Conclusions

In this paper, we demonstrate the effects of energy source depletion on active nematic texture and dynamics by performing fluorescence imaging over 45 h. Such prolonged observation revealed two stages of change in the active nematic. In the first stage, the ATP source of motion was gradually depleted, leading to an overall slow-down in active dynamics, characterised by v_{rms} and active lengthscale. After the driven motion ceased, we observed further textural changes associated with kinesin binding within the network. These results primarily demonstrate the timescales over which active nematic dynamics are significantly affected by ATP depletion in a standard experimental geometry, even with the use of an ATP regeneration system. Constant variation in v_{rms} and active length-scale is a source of error in experimental work and thus, these results may be useful for experimental planning and interpretation of results collected over long timescales.

Acknowledgments

The authors would like to thank the National Science Foundation (NSF) award DMR-1808926 for generous funding.

Disclosure statement

No potential conflict of interest was reported by the author(s).

Funding

The project was also supported by the NSF through the Center of Research Excellence in Science and Technology: Center for Cellular and Biomolecular Machines at the University of California Merced [HRD-1547848] and the Brandeis Biomaterials Facility Materials Research Science and Engineering Center [DMR-2011486].

References

- [1] Sanchez T, Chen D, DeCamp S, et al. Spontaneous motion in hierarchically assembled active matter. *Nature*. 2012;491(7424):431–434. doi: [10.1038/nature11591](https://doi.org/10.1038/nature11591)
- [2] Nedelec FJ, Surrey T, Maggs AC, et al. Self-organization of microtubules and motors. *Nature*. 1997;389(6648):305–308. doi: [10.1038/38532](https://doi.org/10.1038/38532)
- [3] Guillamat P, Ignés-Mullol J, Sagués F. Taming active turbulence with patterned soft interfaces. *Nat Commun*. 2017;8(1):564. doi: [10.1038/s41467-017-00617-1](https://doi.org/10.1038/s41467-017-00617-1)
- [4] Thijssen K, Khaladj D, Aghvami SA, et al. Submersed micropatterned structures control active nematic flow, topology, and concentration. *Proc Natl Acad Sci USA*. 2021;118(38). doi: [10.1073/pnas.2106038118](https://doi.org/10.1073/pnas.2106038118)
- [5] DeCamp SJ, Redner GS, Baskaran A, et al. Orientational order of motile defects in active nematics. *Nat Mater*. 2015;14(11):1110–1115. doi: [10.1038/nmat4387](https://doi.org/10.1038/nmat4387)
- [6] Guillamat P, Ignés-Mullol J, Sagués F. Control of active liquid crystals with a magnetic field. *Proc Natl Acad Sci USA*. 2016;113(20):5498–5502. doi: [10.1073/pnas.1600339113](https://doi.org/10.1073/pnas.1600339113)
- [7] Shendruk TN, Doostmohammadi A, Thijssen K, et al. Dancing disclinations in confined active nematic. *Soft Matter*. 2017;13(21):3853–3862. doi: [10.1039/C6SM02310J](https://doi.org/10.1039/C6SM02310J)
- [8] Giomi L. Geometry and topology of turbulence in active nematics. *Phys Rev X*. 2015;5(3):031003. doi: [10.1103/PhysRevX.5.031003](https://doi.org/10.1103/PhysRevX.5.031003)
- [9] Doostmohammadi A, Shendruk TN, Thijssen K, et al. Onset of meso-scale turbulence in active nematics. *Nat Commun*. 2017;8(1):15326. doi: [10.1038/ncomms15326](https://doi.org/10.1038/ncomms15326)
- [10] Alert R, Casademunt J, Joanny J-F. Active turbulence. *An Rev Cond Mat Phys*. 2022;13(1):143–170. doi: [10.1146/annurev-conmatphys-082321-035957](https://doi.org/10.1146/annurev-conmatphys-082321-035957)
- [11] Tan AJ, Roberts E, Smith S, et al. Topological chaos in active nematics. *Nat Phys*. 2019;15(10):1033–1039. doi: [10.1038/s41567-019-0600-y](https://doi.org/10.1038/s41567-019-0600-y)
- [12] Memarian FL, Khaladj D, Hammar D, et al. Forming, confining, and observing microtubule-based active nematics. *J Vis Exp*. 2023;191(191):e64287. doi: [10.3791/64287-v](https://doi.org/10.3791/64287-v)
- [13] Zhou S, Sokolov A, Lavrentovich OD, et al. Living liquid crystals. *Proc Natl Acad Sci, USA*. 2014;111(4):1265–1270. doi: [10.1073/pnas.1321926111](https://doi.org/10.1073/pnas.1321926111)
- [14] Schnitzer M, Block S. Kinesin hydrolyses one ATP per 8-nm step. *Nature*. 1997;388(6640):386–390. doi: [10.1038/41111](https://doi.org/10.1038/41111)
- [15] Hawkins TL, Sept D, Mogessie B, et al. Mechanical properties of doubly stabilized microtubule filaments. *Biophys J*. 2013;104(7):1517–1528. doi: [10.1016/j.bpj.2013.02.026](https://doi.org/10.1016/j.bpj.2013.02.026)
- [16] Thielicke W, Stamhuis EJ. Pivlab – Towards user-friendly, affordable and accurate digital particle image velocimetry in MATLAB. *J Open Res Software*. 2014;2(1):e30. doi: [10.5334/jors.bl](https://doi.org/10.5334/jors.bl)
- [17] Thielicke W. The flapping flight of birds - Analysis and application [PhD Thesis]. Rijksuniversiteit Groningen; 2014. <http://irs.ub.rug.nl/ppn/382783069>
- [18] Mitchell KA, Tan A, Arteaga J, et al. Fractal generation in a two-dimensional active-nematic fluid. *Chaos*. 2021;31(7):073125. doi: [10.1063/5.0050795](https://doi.org/10.1063/5.0050795)